Polyampholyte model of ion clusters: double-layer interactions in the presence of dissociated simple salt

David Ribar, 1 Clifford E. Woodward, 2 and Jan Forsman 1

¹⁾ Computational Chemistry, Lund University, P.O.Box 124, S-221 00 Lund, Sweden

²⁾School of Physical, Environmental and Mathematical Sciences University College, University of New South Wales, ADFA Canberra ACT 2600, Australia

(*Electronic mail: jan.forsman@compchem.lu.se)

(Dated: November 24, 2025)

We explore interactions between equally charged surfaces, in the presence of simple salt and either neutral or monovalently charged polyampholytes. We consider the possibility of using these charged polymers as crude models of ion clusters. The latter have been hypothesised to form in concentrated aqueous salt solutions, and are possibly related to anomalous underscreening. This phenomenon usually manifests itself by unexpectedly strong and long-ranged effective forces at very high ionic strengths. If ion clusters are formed, they are expected to carry at most a weak net charge. Keeping this in mind, we investigate how polyampholyte chains mediate interactions between charged surfaces. A significant amount of simple salt is also present, in most cases. We highlight that if the charges of the polyampholytes are unevenly distributed, there is a polarisation response that in turn can generate very strong and long-ranged surface forces, even at rather high concentrations of simple salt. Aside from their possible relevance to ion clusters and underscreening phenomena, these results also suggest the possibility of tailoring synthetic polyampholytes, in order to regulate colloidal stability.

I. INTRODUCTION

Using simple salts to tune the stability of colloidal dispersions containing charged particles is a long-established and theoretically well-grounded process^{1–13}. For aqueous systems with monovalent ions, mean-field theories provide reliable predictions at low and intermediate concentrations. A central outcome of such treatments is the Debye screening length, λ_D , which characterizes the effective range of electrostatic interactions in an ionic medium. Increasing the salt concentration enhances ionic screening, thereby reducing λ_D ($\sim 1/\sqrt{c}$).

Surprisingly, recent measurements using the Surface Force Apparatus (SFA) have revealed a non-monotonic trend: beyond a threshold concentration (typically near 1 M) the range of effective repulsion between charged surfaces *increases* with added salt^{14–17}. Similar trends have been reported in studies of colloidal stability¹⁸ and thin films¹⁹, though conflicting results also exist²⁰. Despite numerous theoretical efforts to rationalise these observations^{21–32}, the molecular origin of this anomalous behaviour remains unresolved.

One proposed mechanism involves the formation of ionic clusters, which would alter the effective free ion population and lead to unexpectedly long-ranged interactions at high ionic strengths $^{14,29,30,32-35}$. Experimental evidence supporting ion clustering at high concentrations has been reported in previous studies $^{36-43}$.

In this work, we examine surface forces in aqueous environments containing (mainly) linear ionic clusters that crudely mimic the ionic aggregates that may form in reality. We use an implicit solvent representation, where water enters only through its dielectric constant ($\varepsilon_r = 78.3$), and where some of the ions are connected to form linear

aggregates. These clusters either carry a univalent net charge, or are overall neutral. A population of simple salt (at least 100mM) is also included in the (model) solution, keeping in mind that even if ion clusters are formed, one would anticipate a remaining fraction of dissociated ions. These systems are analysed using classical polymer Density Functional Theory, cDFT. We demonstrate that such "clustered electrolytes" can generate remarkably strong repulsive forces between similarly charged surfaces at short and intermediate separations, especially if the polyampholytes have a heterogeneous charge distribution, allowing a strong polarisation response.

II. MODEL AND THEORY

The cartoon in Figure 1 illustrates our two main models, which contain (monodisperse) ion clusters plus simple salt.

Figure 1 shows monovalent linear 11-mer polyampholytes, which we denote as a 11:11 salt, keeping in mind that this does *not* imply that the species are multivalent. Indeed, we will restrict our models to contain only monovalent or net neutral polyampholytes. The single charged monomers are connected by bonds with a fixed length, b, but with full rotational freedom. While we primarily use linear architectures for these polyampholytes, some comparisons with results from branched chain models are made in the Appendix. We find that, at least for alternating charge models, cDFT predictions with linear and branched chains agree almost quantitatively.

We shall consider polyampholytes with two different charge arrangements: *alternating* charges and *block* charges. Even degrees of polymerisation give neutral

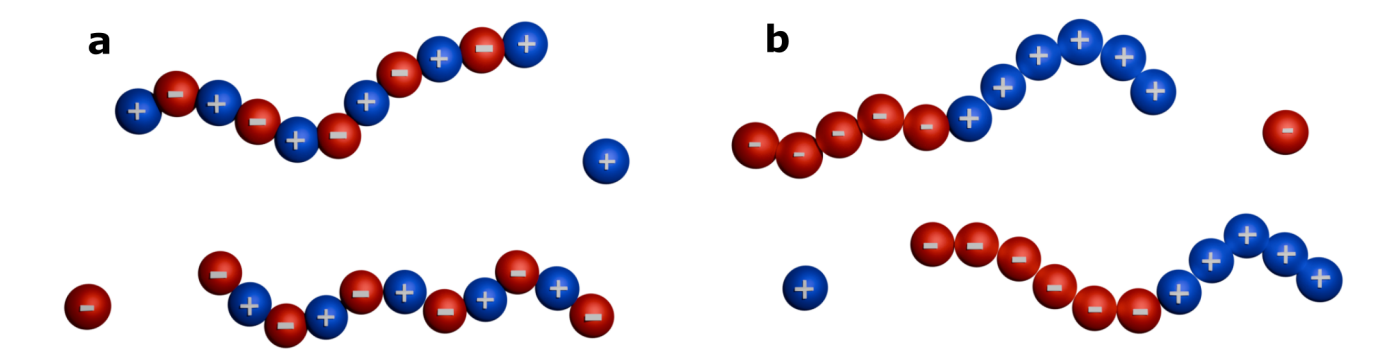


Figure 1: An illustration of a (monovalent) 11:11 polyampholyte plus 1:1 simple salt. $\bf a$ The alternating charge model. $\bf b$ The block charge model.

polyampholytes, whereas odd degrees of polymerisation leads to a monovalent polyampholyte salt. We use r to denote the degree of polymerisation (the number of monomers per polyampholyte chain). It should be noted that in a "real" solution, the block charge model might be prone to folding and flocculation at low concentrations of simple salt. However, these polymers are likely to be soluble at high ionic strengths.

Unless otherwise specifically stated, surface interactions will be evaluated for like-charged walls with a surface charge density of $\sigma_s = -0.014286e/\text{Å}^2$. This is close to estimated values for mica in salt solution⁴⁴, which is used in SFA experiments. The calculations are performed using polymer-cDFT, which accounts for hard-sphere exclusion between particles and with a mean-field treatment of Coulomb interactions.

Non-bonded interactions between monomers are described by the pair potential $\phi_{ij}(r)$, defined as

$$\beta \phi_{ij}(r) = \begin{cases} \infty; & r \le d \\ l_B \frac{Z_i Z_j}{r}; & r > d \end{cases} , \tag{1}$$

where $\beta=(k_BT)^{-1}$ is the inverse thermal energy, and d denotes the monomer diameter. The Bjerrum length is $l_B\approx 7.16$ Å, and Z_i and Z_j denote the valencies of monomers i and j (|Z|=1 throughout this work). We use n_+ and n_- to denote densities of positive and negative polyampholyte monomers, whereas n_c and n_a are the concentrations of dissociated cations and anions.

We consider a system consisting of two infinite, rigid, and planar surfaces separated by a distance h. Each surface carries a uniform charge density and the surfaces are immersed in the model mixture, and the inter-surface distance h is varied. The system is described within the grand canonical ensemble, implying that the confined fluid remains in chemical equilibrium with a bulk reservoir of infinite extent. For each separation, the equilibrium (minimal) free energy is determined, and the resulting osmotic pressure is evaluated either by numerically differentiating the free energy or via the contact

densities of monomers at the surfaces. All polymer configurations are included following Boltzmann weighting, assuming that density variations occur solely in the direction perpendicular to the walls⁴⁵.

In a completely ideal bulk polymer solution, where the only constraints are the intramolecular bonds and no intermolecular interactions or external potentials are present, the free energy \mathcal{F}_p^{id} for an r-mer can be written exactly as

$$\beta \mathcal{F}^{(id)} = \int N(\mathbf{R}) \left(\ln[N(\mathbf{R})] - 1 \right) d\mathbf{R} + \beta \int N(\mathbf{R}) V_b(\mathbf{R}) d\mathbf{R},$$
(2)

where $\mathbf{R} = (\mathbf{r}_1, ..., \mathbf{r}_r)$ denotes a polymer configuration, and $N(\mathbf{R})$ is the distribution function such that $N(\mathbf{R})d\mathbf{R}$ gives the number of polymer molecules with configurations in the range $[\mathbf{R}, \mathbf{R} + d\mathbf{R}]$. The bond potential between adjacent monomers is denoted $V_b(\mathbf{R})$. In this work, we assume bonds of fixed length, i.e.

$$e^{-\beta V_b(\mathbf{R})} \propto \prod \delta(|\mathbf{r}_{i+1} - \mathbf{r}_i| - b),$$
 (3)

where we recall that b is the bond length, and $\delta(x)$ is the Dirac delta function. For the simple 1:1 salt, the corresponding ideal free energy, F_s , naturally lacks the polymer components:

$$\beta F_s^{id} = \int n_c(\mathbf{r}) \left(\ln[n_c(\mathbf{r})] - 1 \right) d\mathbf{r} + \int n_a(\mathbf{r}) \left(\ln[n_a(\mathbf{r})] - 1 \right) d\mathbf{r}.$$
(4)

In order to avoid complicated indexing, we will limit our cDFT description to models of net monovalent polyampholyte chains (plus simple salt). The simplification that ensue for net neutral polyampholytes should be obvious.

The Helmholtz free energy for the bulk polyampholyte salt model can be expressed as

$$\mathcal{F}(V, T, N_{+}, N_{-}) = \sum_{i=\pm} \mathcal{F}^{(id)} + F_{s}^{id} + \mathcal{F}^{(ex)}_{HS}(n_{+}, n_{-}, n_{c}, n_{a}) + \mathcal{U}.$$
(5)

Here, i distinguishes between two oppositely charged polymer species with alternating monomer charges. Cationic chains start and end with positive monomers, whereas anionic chains terminate with negative ones. In the bulk, both species contribute identically to the ideal free energy, while in confined or heterogeneous environments their free energies differ. Excluded-volume effects are represented by $\mathcal{F}_{HS}^{(ex)}$, which depends on the total cationic and anionic monomer densities, n_+ and n_- , as

well as the densities of the unconnected (simple salt) ions, n_c and n_a . This contribution is estimated using the Generalised Flory–Dimer (GFD) approach⁴⁶, which accounts for differences in excluded volume between end monomers, dissociated monomers (simple salt ions), and inner monomers. All electrostatic terms are contained in \mathcal{U} and are treated within the mean-field approximation.

In the slit geometry, we employ the grand potential Ω , related to \mathcal{F} by the Legendre transformation

$$\Omega(V, T, \mu_{+}, \mu_{-}; [n_{+}, n_{-}, n_{c}, n_{a}\sigma])A^{-1} = \mathcal{F}(V, T; [n_{+}, n_{-}, n_{c}, n_{a}, \sigma, \Psi_{D}])A^{-1}
+ \sum_{i=\pm} \int (V_{ex}(z) - \mu_{i})N_{i}(z_{1}..., z_{r})dz_{1}, ..., dz_{r}
+ \int (V_{ex}(z) - \mu_{c})n_{c}(z)dz + \int (V_{ex}(z) - \mu_{a})n_{a}(z)dz,$$
(6)

where z denotes the coordinate perpendicular to the surfaces, A is the surface area, and Ψ_D is the Donnan potential that ensures overall electroneutrality. The total free energy \mathcal{F} encompasses contributions from configurational entropy, excluded-volume interactions, and meanfield electrostatics, including the wall-wall interaction. The chemical potentials of cationic and anionic chains are represented by μ_{+} and μ_{-} , respectively, and the notation for simple ions is similar: μ_c and μ_a . The surface interaction potential $V_{ex}(z)$ accounts for non-electrostatic exclusion and is purely steric, being zero within the accessible region (d/2 < z < (h - d/2)) and infinite elsewhere. The equilibrium grand potential, $\Omega_{eq}(h)$, is obtained by numerical minimisation using Picard iteration. Defining $g_s(h) \equiv \Omega_{eq}/A - p_b h$, where p_b is the bulk pressure, the net interaction free energy is given by $\Delta g_s \equiv g_s(h) - g_s(h \to \infty)$. The tail of this interaction is assumed to be an exponential decay (which is confirmed numerically below). We then set $g_s(h \to \infty) \approx g_s(h_0)$, where h_0 is a surface separation larger than 15 decay lengths (as estimated from the fit).

Further details of the numerical algorithm are available in 47,48, but a short summary is provided here. Due to planar symmetry and the mean-field approximation, densities and interactions can be integrated along the

(x,y) directions parallel to the surfaces while maintaining electroneutrality. Accordingly, only z-dependent quantities are retained within the slit region. The laterally integrated Coulomb interaction between two monomers with valencies Z_{γ} and Z_{δ} at positions z and z' is given by $\beta\phi(z,z')=-2\pi Z_{\gamma}Z_{\delta}l_B|z-z'|$. We introduce $\lambda_{hs}\equiv \partial \mathcal{F}_{HS}^{(ex)}/\partial n_{+}=\partial \mathcal{F}_{HS}^{(ex)}/\partial n_{-}$, noting that cationic and anionic monomers are of equal size.

Polymer configurations are treated within a classical density functional framework under mean-field weighting. The equilibrium monomer density is expressed in terms of auxiliary propagator functions c(i,z), where i labels the monomer along the chain. Separate propagators, $c_+(i,z)$ and $c_-(i,z)$, are introduced for cationic and anionic chains, respectively. For cationic polymers, the contribution to the total monomer density n'(z) at position z reads

$$n'(z) = e^{\beta \mu_+} \sum_{i=1}^{r} c_+(i, z) * c_+(r+1-i, z), \qquad (7)$$

where the prime indicates that only positively charged chains are considered. Propagator relationships will of course depend on the polymer architecture. For instance, if the chains have alternating charges, then the recursive relation governing the auxiliary functions is

$$c_{+}(i,z) = e^{\beta \lambda_{hs}(z)/2} \rho_{+}(z)^{(-1)^{(i-1)}} \int c_{+}(i-1,z') T(z,z') \rho_{+}(z')^{(-1)^{i}} dz', \tag{8}$$

for i > 1, and

$$c_{+}(1,z) = e^{\beta \lambda_{hs}(z)/2} \rho_{+}(z),$$
 (9)

where $\rho_{+}(z) \equiv e^{-\beta e \Psi(z)/2}$ and $\Psi(z)$ is the local electro-

static potential (including Ψ_D). The kernel T(z, z') imposes the fixed bond length constraint and includes a

normalisation factor:

$$T(z, z') = \frac{\Theta(|z - z'| - b)}{2b}.$$
 (10)

Anionic chains are treated analogously, and for unconnected ions there is no need for auxiliary functions, as there are no bond integrals 48 . To ensure stable convergence, conservative Picard iterations are applied—mixing a small fraction of updated densities with the previous ones—and the Donnan potential is simultaneously adjusted to maintain global electroneutrality. Convergence is achieved when the maximum relative change between successive iterations falls below 10^{-7} at all points.

In order to facilitate direct comparisons with SFA/AFM measurements, we will assume the validity of the Derjaguin Approximation, and present interaction free energies as force per radius, F/R.

III. RESULTS. 1. NEUTRAL POLYAMPHOLYTES

We will initially explore surface interactions in the presence of net neutral polyampholytes, i.e. those composed of an even number of charged monomers.

A. Ideal dimers (zwitterions)

We begin by establishing the dipolar response of a fluid of ion pairs with opposite charges bonded at a distance b without hard cores. We denote these as "ideal dimers".

1. Dielectric response, no salt

We can evaluate the impact that these ideal dimers have on the overall dielectric response of the system⁴⁹ by calculating the net pressure between oppositely charged surfaces. In order to avoid saturation effects, that are likely to vanish in the presence of added salt anyway, we will in this case model these surfaces as weakly charged, $|\sigma_s| = 0.001e/\text{ Å}^2$. Since there is no salt present, these oppositely charged walls will experience a constant attraction at long range, with a net pressure that is inversely proportional to the dielectric constant of the medium that separates them. In the presence of zwitterions, this dielectric constant will shift from the reference value ε_w , in the absence of dipoles, to some higher value: ε . Hence, the ratio between these attractive pressures will directly give us the ratio $\varepsilon/\varepsilon_w$. The results, for various zwitterion concentrations, and charge separation values (b), are collected in Figure 2a. In agreement with experimental findings 50,51 , there is a linear dependence on concentration.

2. Ideal dimers and ideal salt

We now consider interactions between equally charged surfaces with the standard charge density of σ_s = $-0.014286e/Å^2$), in the presence of 1900 mM ideal dimers and 100 mM of a simple 1:1 (ideal) salt. These concentrations are commensurate with a salt solution which is overall 2M but where a substantial degree of ion pairing occurs, leaving only 100 mM of dissociated salt. We note that, in this case, no charged species will carry a hard core. In Figure 2b, we see the effect of the zwitterions on the double layer repulsion, which is stronger when the zwitterions are present. This response is also affected by the bond-length of the dimers. From meanfield theory, we expect that the Debye length, λ_D , will scale as the square root of the dielectric constant, ε . Extracting the appropriate values from Figure 2a we find $\varepsilon(b = 4 \text{ Å}, 1900mM)/\varepsilon_w \approx 1.55 \text{ and } \varepsilon(b = 8)$ Å, 1900mM)/ $\varepsilon_w \approx 3.20$. This implies that:

$$\frac{\lambda_D(\text{b=4 Å,1900 mM})}{\lambda_D(\text{no dipoles})} \approx \sqrt{1.55} \approx 1.25$$
 (11)

and:

$$\frac{\lambda_D(\text{b=8 Å,1900 mM})}{\lambda_D(\text{no dipoles})} \approx \sqrt{3.20} \approx 1.79.$$
 (12)

These ratios can be directly compared with the observed electrostatic decay lengths, evaluated from inverted slopes of the logarithm of the net pressure, i.e. the dashed lines in Figure 2c. Denoting the inverse of these linearly fitted slopes by α , we obtain

$$\frac{\alpha(\text{no dipoles})}{\alpha(\text{b=4 Å,1900 mM})} \approx 1.26$$
 (13)

and

$$\frac{\alpha (\text{no dipoles})}{\alpha (\text{b=8 Å,1900 mM})} \approx 1.84. \tag{14}$$

Given the excellent agreement between these sets of values, we conclude that the increased double layer repulsion observed in the presence of the dimers can be fully ascribed to their dipolar response. This response, which obviously is quite strong, is often neglected in theoretical considerations of ion pairing, and its impact on surface forces.

B. Neutral polyampholytes plus simple salt. The "gradual growth" of neutral ion clusters.

As stated earlier, the above solution can be viewed as a crude model wherein a 2 M 1:1 salt solution undergoes partial ion pairing, leaving 100 mM of dissociated salt. Let us now explore what happens if the clusters that are formed are larger. Specifically, we will assume that r-mers are now formed from the 2 M 1:1 solution, with 100

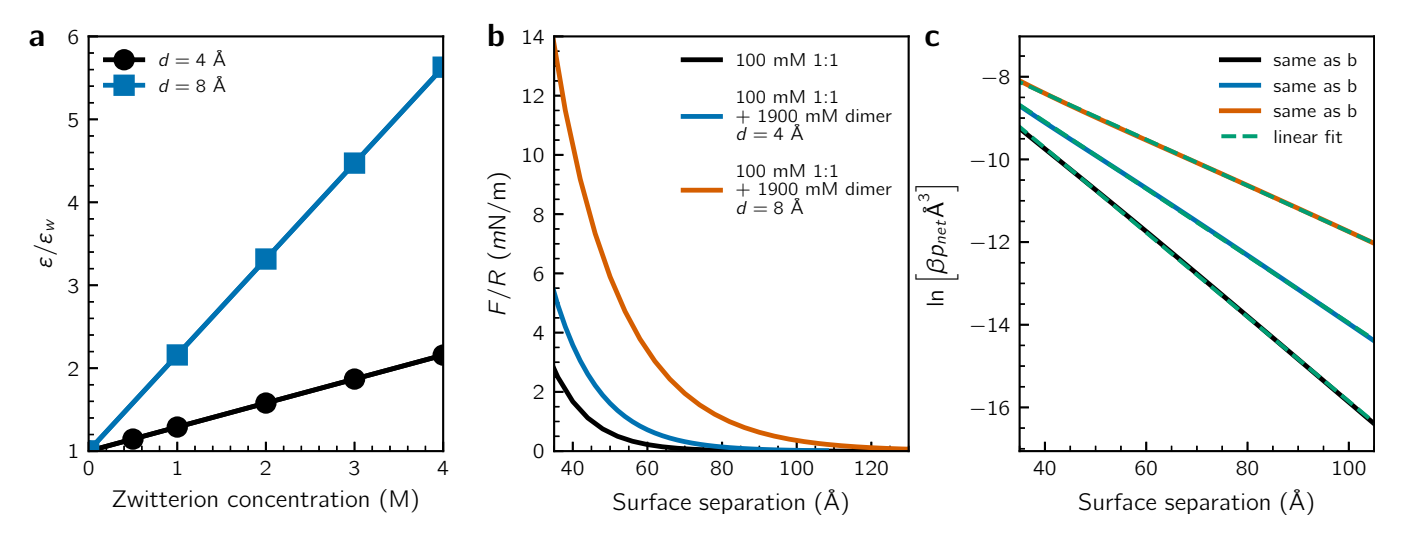


Figure 2: **a** The dependence of $\varepsilon/\varepsilon_w$ with zwitterion concentration, for two different choices of b. Calculated data are indicated by symbols. The lines are linear regression fits. **b** Force per radius values between equally charged surfaces, in the presence of 1900 mM zwitterions and 100 mM simple 1:1 salt (no excluded volume). **c** The corresponding logarithm of the net pressure.

mM free salt remaining. For instance, with r=10, we will have a mixture of 100 mM 1:1 salt and 380 mM of neutral 10-mers. Furthermore, we will assume all species have hard cores of diameter d=4 Å in our ongoing calculations. Connected monomers in the r-mers are separated by a bond-length of b=6 Å.

1. Chains with alternating charges

In Figure 3a we show the surface interaction free energies for systems with neutral r-mers containing alternating charges. As in the earlier case for ion pairs and simple salt, the presence of the neutral clusters leads to a significantly stronger repulsion when compared with the simple salt only solution. This is due to the enhanced dielectric response of the ionic chains. On the other hand, an increase of r from 10 to 20, even with a concomitant drop of the polymer concentration, has essentially no impact on the net surface interaction. This indicates the polarization response of the chains depends primarily on the number of bonded ions, rather than the concentration of the clusters.

2. Chains with block charge structure

The corresponding contribution from polyampholytes that are composed of two *blocks* of opposing charge is *enormous*. This is illustrated in Figure 3b. Such a complete charge separation is arguably an upper limit in "real" clusters, although one would expect a significant polarisation response in the vicinity of the charged surfaces (a more realistic model, to be explored in future work) At this stage, we note that the double layer forces

acting in these systems are quite sensitive to the internal structure of the polyampholytes, i.e. our model of ion clusters. In contrast to the case with alternating charges, we here see a strong dependence on polymer length, r. An increased degree of polymerisation leads to a stronger and more long-ranged interaction when the chains have a block structure. This is not surprising, since the block architecture creates larger dipole moments, due to an increased separation of larger charged blocks within each cluster. Both the separation and and size of the charged blocks will increase approximately with the inverse of concentration. This means the dielectric response will also increase with the inverse concentration.

We have already mentioned that in a bulk solution, spontaneously formed ion clusters are unlikely to resemble block chains. Nevertheless, near a strongly charged surface, this is perhaps not a totally unrealistic description. Moreover, these predictions, of surface forces with a truly remarkable range and strength, even with short polymer lengths, might imply novel applications of synthesized polyampholytes with a block charge structure.

Another property that might be relevant, but is neglected in the current work, is polydispersity effects. Real solutions of clustering ions will contain clusters of varying size, some of which are likely to be neutral, whereas others are weakly charged. Polydispersity effects are beyond the scope of the current study, but will be investigated in future work.

IV. RESULTS. 2. MONOVALENT POLYAMPHOLYTES PLUS SIMPLE SALT

In a recent work⁵², we demonstrated that monovalent polyampholyte salts generate much stronger repul-

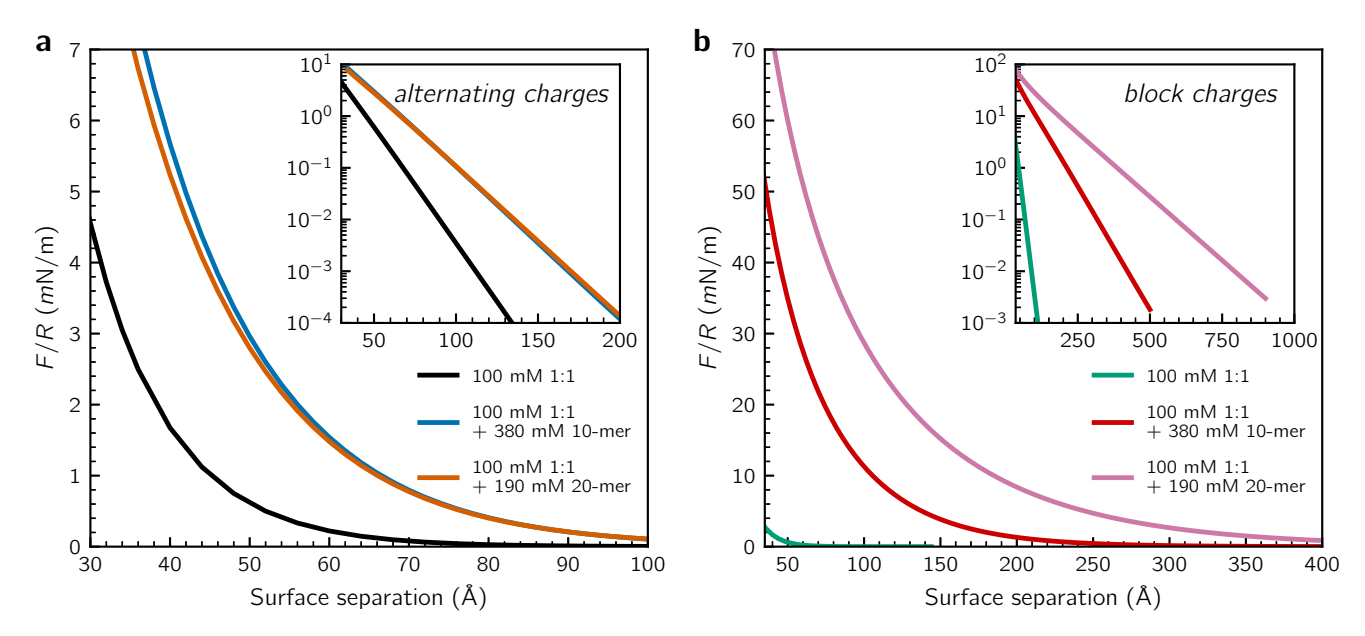


Figure 3: Interactions between equally charged surfaces, in the presence of neutral r-mer polyampholytes, and 100 mM simple 1:1 salt (including excluded volume). For a given polymer length r, the polyampholyte concentration is chosen in a way that is commensurate with clustering of a 2 M simple salt solution. The case of a pure 100 mM simple salt solution is shown as reference. The insert presents the logarithm of the F/R data. a The chains are composed of monomers with an alternating charge structure. b The chains are composed of monomers with a block charge structure.

sive surface forces, than a simple 1:1 salt at the same salt concentration. We have also established (above) how the presence of neutral "ion clusters", as modelled by our polyampholyte description, also leads to a substantially increased repulsion. Here, we will explore the surface force response to the presence of monovalent charged polyampholytes in addition to simple salt. We note that earlier simulation work has established that ion clusters tend to be either neutral, or weakly charged ^{29,32}. This is also expended on physical grounds, since the formation of highly charged clusters would be associated with a considerable electrostatic free energy cost.

In Figure 4a, we see how the response to the addition of monovalent polyampholyte chains, with and alternating charge is considerably weaker than when these are net neutral (cf. Figure 3a). Longer chains, at a constant monomer concentration, do increase the range somewhat, but the net increase of the repulsion is hardly dramatic.

On the other hand, when the polyampholytes have a block charge structure, they generate an enormous repulsion, even at high ionic strength and with relatively short chains. This is illustrated in Figure 4b, where we also note that the range and the strength of the surface interaction increase quite substantially, when such polymers are added. As we have seen earlier, this is in turn related a strong polarisation of molecules with such an architecture.

The slow decay of the electrostatic potential, obtained in the presence of monovalent *block* charge polyampholytes, can also be illustrated by density profiles of charged species. In Figure 4c, we see how the polymer presence generate a remarkable extension to the thickness of the "diffuse" layer, i.e. the electrostatic potential decays much slower than in a corresponding salt solution without polyampholytes. A seemingly peculiar behaviour is that the anionic monomers approaches the mid plane value from *above*, even though the surfaces carry a negative charge. This is not due to overcharging, as is clear from the fact that the dissociated anions displays an opposite trend. The behaviour should rather be considered a consequence of connectivity, since the cationic part of the polymers are strongly adsorbed at the walls.

A. Modelling the "gradual growth" of ion clusters with a *block* charge structure

Let us revisit a process similar to that we considered for neutral polyampholyte chains. We imagine a 2 M 1:1 salt solution in which monovalent block charge 25:25 clusters are formed, to a gradually increasing extent. This then suggests a gradual drop of the remaining "free" ions, which together form a 1:1 salt. The corresponding cDFT prediction of surface forces are displayed in Figure 5. As before, we find a dramatic impact by the presence of block polyampholytes. While we would expect that clusters of fully separated blocks of charge are unlikely, even at high ionic strength, the results may be viewed as a useful limiting case, at the opposite extreme to that of alternating charges. We would expect that alternating

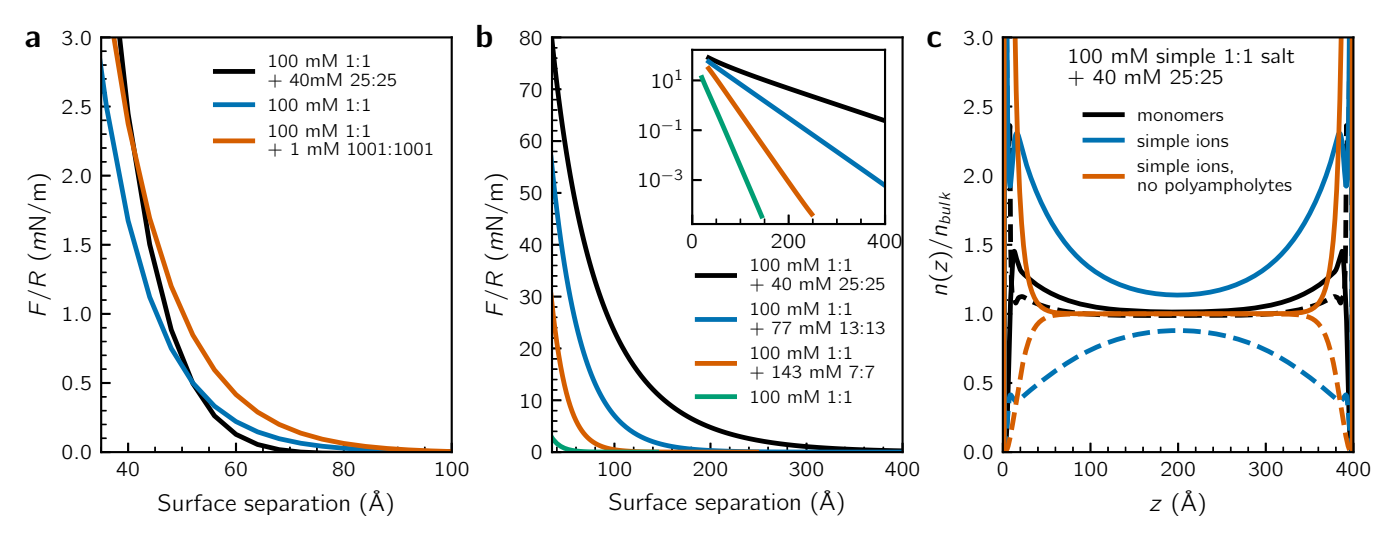


Figure 4: a Surface forces, in the presence of 100 mM pure 1:1 salt solutions, as well as in mixtures of 100 mM simple 1:1 plus added monovalent 25:25 (40 mM) or 1001:1001 (1 mM) salt. The concentrations of the polyampholyte salt are commensurate with an overall monomer concentration of 2000 mM. The alternating charge model has been adopted for the polyampholyte chains. b Same as a, but for 40 mM monovalent 25:25 salt using the block charge structure. c Density profiles, at h = 400 Å, in solutions containing 100 mM simple 1:1 salt and 40 mM 25:25. Full lines denote the cations, while the dashed lines denote the anions.

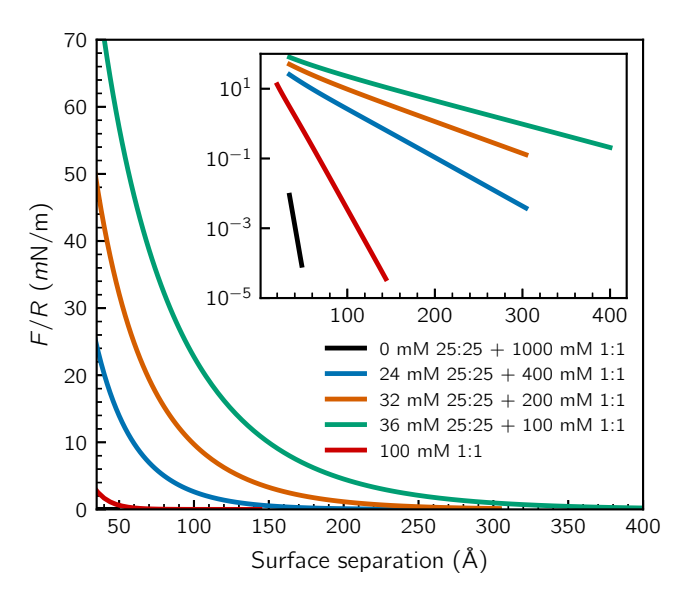


Figure 5: Surface forces, in the presence of pure 1:1 salt solutions, and in mixtures of simple 1:1 and monovalent 25:25 salt. In the latter cases, the *block* charge model has been adopted. With one exception, the total concentration of positive, as well as negative, charged spheres in the bulk is 2 M. The case of a pure 100 mM simple salt solution is shown as reference.

clusters should be preferred far from the charged surface, but the field from highly charged surfaces is expected to generate polarized (block-like) clusters in their vicinity. We expect that in a real scenario that surface forces will display a behaviour between these two extremes.

V. CONCLUSIONS

We have demonstrated that a commonly adopted simplification, where ion cluster effects on surface forces are accounted for simply by the concomitant drop of the dissociated (free) ion concentration, may turn out to be inaccurate. This is because the ion clusters themselves contribute substantially to the interactions. Neutral clusters, modelled as chains of alternating charge (which may be prevalent due to the small Coulombic cost of creating them²⁹) can have a significant effect due to their dielectric response. Moreover, the massive dipolar response we have observed for block architectures suggests that perhaps even a modest anisotropy of the ion cluster charge distribution may have a strong impact on the interaction between charged surfaces.

As already mentioned, our current models would be nefit from the incorporation of polydispersity, as well as the ability of the chains to alter the connectivity in response to the presence of fields. These effects will be accounted for in future work, utilising cDFT formulations that we have previously developed for similar systems⁵³.

We have mainly discussed the polyampholytes as crude models of ion clusters, but it should be noted that our findings have broader implications. Given a solution of relatively high ionic strength, it would be quite feasible to synthesize polyampholytes with a block charge structure, for instance using established biochemical approaches, and suitably chosen peptides. Such block polyampholytes could then serve as stabilisers of colloidal dispersions, and their impact might be modulated by appropriate adjustments of pH. Moreover, the strong dipolar response that we observe is likely to be relevant in solutions containing

"patchy" colloidal particles, such as proteins.

ACKNOWLEDGMENTS

J.F. acknowledges financial support by the Swedish Research Council.

AUTHOR DECLARATIONS

Conflict of Interest

The authors have no conflicts to disclose.

Author Contributions

David Ribar: Conceptualization, Formal Analysis, Validation, Visualization, Writing/Review & Editing. Clifford Woodward: Conceptualization, Methodology, Writing/Review & Editing. Jan Forsman: Conceptualization, Formal Analysis, Funding Acquisition, Methodology, Software, Supervision, Writing/Original Draft Preparation, Writing/Review & Editing.

DATA AVAILABILITY STATEMENT

The data that support the findings of this study are available from the corresponding author upon reasonable request.

Appendix A: Branched polyampholyte structure

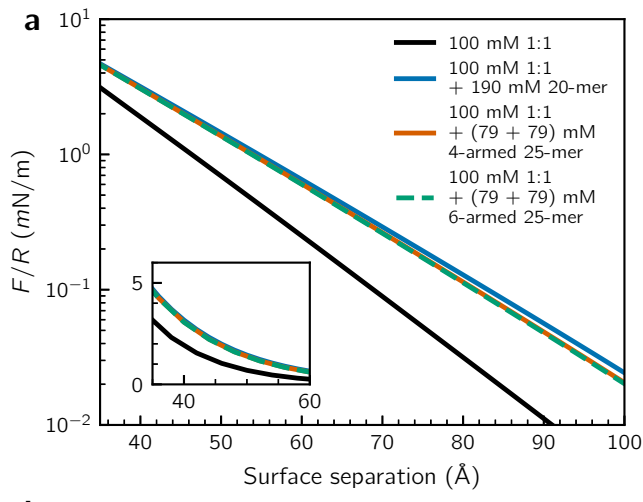
1. Branched neutral chains (alternating charge)

It turns out that, at least within the mean-field approximation, there is no difference of practical importance between the multipole response from linear or branched chain, at a similar degree of polymerisation. This is illustrated in Figure 6a.

This lends support to the hypothesis that a linear polymer model of ion clusters, which might appear unrealistically "stretched", actually is able to incorporate the most salient physics, at least for models of neutral polyampholytes with alternating charges. In other words, the overall multipole is quite similar (and significant), from models using branched polymer architectures.

2. Branched monovalent chains (alternating charge)

Here we evaluate effects from making the charged monovalent polymer models more "compact", and arguably more cluster-like, by using branched (star-like)



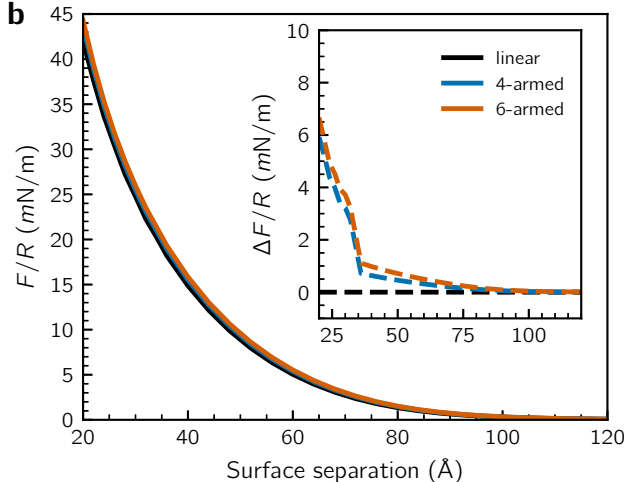


Figure 6: a Interactions between equally charged surfaces, in the presence of X mM r:r polyampholytes, and 100 mM simple 1:1 salt. For a given degree of polymerisation r, X is chosen in a way that is commensurate with clustering of a 2 M simple salt solution. However, a neutral branched chain also contains an uncharged central monomer. Moreover, the branched chains form a mixture of polymers with cation/anion end charges (although all branches are overall electroneutral). This means that (say) a 25-mer cluster contains 24 charges and that there are two different versions of such a neutral cluster. **b** Surface forces, in the presence of a mixture of 10 mM simple 1:1 salt and 40 mM monovalent 25:25 salt (alternating charges). Apart from results for linear chains, we provide results for branched (star-like) 25-mer polyampholyte models, with 4 and 6 "arms". The insert present the difference from the linear surface forces, to highlight the structure effect.

backbone descriptions. As we see in Figure $6\mathbf{b}$, the branched chains mediate stronger but more short-ranged surface forces. In the displayed case (40 mM monovalent 25-mers plus 10 mM 1:1 salt), the threshold separation is

about 70 Å, below which the branched model produces a stronger repulsion.

REFERENCES

- ¹G. Gouy, J. Phys. **9**, 457 (1910).
- ²D. L. Chapman, "LI. A contribution to the theory of electrocapillarity," Philosophical Magazine Series 6 **25**, 475–481 (1913).
- ³B. V. Derjaguin and L. Landau, "Theory of the stability of strongly charged lyophobic sols and of the adhesion of strongly charged particles in solutions of electrolytes," Acta Phys. Chim. URSS 14, 633–662 (1941).
- ⁴E. J. W. Verwey and J. T. G. Overbeek, *Theory of the Stability of Lyophobic Colloids* (Elsevier Publishing Company Inc., Amsterdam, 1948).
- ⁵F. Oosawa, *Polyelectrolytes* (Marcel Dekker, New York, 1971).
- ⁶L. Guldbrand, B. Jönsson, H. Wennerström, and P. Linse, "Electrical double layer forces, A Monte Carlo study." J. Chem. Phys. 80, 2221 (1984).
- ⁷R. Kjellander and S. Marcelja, "Interaction of charged surfaces in electrolyte solutions," Chem. Phys. Lett. **127**, 402–407 (1986).
- ⁸S. Nordholm, "Generalized van der waals theory. xii. application to ionic solutions," Aust. J. Chem. 37, 1 (1984).
- ⁹S. Nordholm, Chem. Phys. Lett. **105**, 302 (1984).
- ¹⁰J. N. Israelachvili, *Intermolecular and Surface Forces, 2nd Ed.* (Academic Press, London, 1991).
- ¹¹F. A. Evans and H. Wennerström, The colloidal domain: where Physics, Chemistry, Biology and Technology meet (VCH Publishers, New York, 1994).
- ¹²C. Holm, P. Kekicheff, and R. Podgornik, *Electrostatic Effects in Soft Matter and Biophysics* (Kluwer Academic Publishers, Dordrecht, 2001).
- ¹³J. Forsman, "A simple correlation-corrected poisson-boltzmann theory." J. Phys. Chem. B 108, 9236 (2004).
- ¹⁴M. A. Gebbie, M. Valtiner, X. Banquy, E. T. Fox, W. A. Henderson, and J. N. Israelachvili, "Ionic liquids behave as dilute electrolyte solutions," PNAS 110, 9674–9679 (2013), https://www.pnas.org/doi/pdf/10.1073/pnas.1307871110.
- ¹⁵M. A. Gebbie, H. A. Dobbs, M. Valtiner, and J. N. Israelachvili, "Long-range electrostatic screening in ionic liquids," PNAS 112, 7432–7437 (2015), https://www.pnas.org/doi/pdf/10.1073/pnas.1508366112.
- ¹⁶A. M. Smith, A. A. Lee, and S. Perkin, "The electrostatic screening length in concentrated electrolytes increases with concentration," J. Phys. Chem. Lett. 7, 2157–2163 (2016), https://doi.org/10.1021/acs.jpclett.6b00867.
- ¹⁷Y. K. C. Fung and S. Perkin, "Structure and anomalous underscreening in ethylammonium nitrate solutions confined between two mica surfaces," Faraday Discuss. **246**, 370–386 (2023).
- ¹⁸H. Yuan, W. Deng, X. Zhu, G. Liu, and V. S. J. Craig, "Colloidal systems in concentrated electrolyte solutions exhibit re-entrant long-range electrostatic interactions due to underscreening," Langmuir 38, 6164–6173 (2022), https://doi.org/10.1021/acs.langmuir.2c00519.
- ¹⁹P. Gaddam and W. Ducker, "Electrostatic screening length in concentrated salt solutions," Langmuir 35, 5719–5727 (2019), https://doi.org/10.1021/acs.langmuir.9b00375.
- ²⁰S. Kumar, P. Cats, M. B. Alotaibi, S. C. Ayirala, A. A. Yousef, R. van Roij, I. Siretanu, and F. Mugele, "Absence of anomalous underscreening in highly concentrated aqueous electrolytes confined between smooth silica surfaces," J. Colloid Interface Sci. 622, 819–827 (2022).
- ²¹A. A. Lee, C. S. Perez-Martinez, A. M. Smith, and S. Perkin, "Scaling analysis of the screening length in concentrated electrolytes," Phys. Rev. Lett. **119**, 026002 (2017).
- ²²F. Coupette, A. A. Lee, and A. Härtel, "Screening Lengths in Ionic Fluids," Phys. Rev. Lett. **121**, 075501 (2018).

- ²³B. Rotenberg, O. Bernard, and J.-P. Hansen, "Underscreening in ionic liquids: a first principles analysis," J. Phys. Condens. Matter 30, 054005 (2018).
- ²⁴R. Kjellander, "A multiple decay-length extension of the debyehückel theory: to achieve high accuracy also for concentrated solutions and explain under-screening in dilute symmetric electrolytes," Phys. Chem. Chem. Phys. **22**, 23952–23985 (2020).
- ²⁵S. W. Coles, C. Park, R. Nikam, M. Kanduc, J. Dzubiella, and B. Rotenberg, "Correlation length in concentrated electrolytes: Insights from all-atom molecular dynamics simulations," J. Phys. Chem. B **124**, 1778–1786 (2020), https://doi.org/10.1021/acs.jpcb.9b10542.
- ²⁶J. Zeman, S. Kondrat, and C. Holm, "Bulk ionic screening lengths from extremely large-scale molecular dynamics simulations," Chem. Commun. 56, 15635–15638 (2020).
- ²⁷P. Cats, R. Evans, A. Härtel, and R. van Roij, "Primitive model electrolytes in the near and far field: Decay lengths from DFT and simulations," J. Chem. Phys. **154**, 124504 (2021), https://pubs.aip.org/aip/jcp/article-pdf/doi/10.1063/5.0039619/14014384/124504_1_online.pdf.
- ²⁸E. Krucker-Velasquez and J. W. Swan, "Underscreening and hidden ion structures in large scale simulations of concentrated electrolytes," The Journal of Chemical Physics 155, 134903 (2021), https://pubs.aip.org/aip/jcp/article-pdf/doi/10.1063/5.0061230/16045961/134903_1_online.pdf.
- ²⁹A. Härtel, M. Bültmann, and F. Coupette, "Anomalous underscreening in the restricted primitive model," Phys. Rev. Lett. 130, 108202 (2023).
- ³⁰G. R. Elliott, K. P. Gregory, H. Robertson, V. S. Craig, G. B. Webber, E. J. Wanless, and A. J. Page, "The known-unknowns of anomalous underscreening in concentrated electrolytes," Chemical Physics Letters 843, 141190 (2024).
- ³¹J. Forsman, D. Ribar, and C. E. Woodward, "An efficient method to establish electrostatic screening lengths of restricted primitive model electrolytes," Phys. Chem. Chem. Phys., DOI: 10.1039/D4CP00546E (2024).
- ³²D. Ribar, C. E. Woodward, and J. Forsman, "Solvent-induced ion clusters generate long-ranged double-layer forces at high ionic strengths," Soft Matter 21, 5562-5572 (2025).
- ³³K. Ma, J. Forsman, and C. E. Woodward, "Influence of ion pairing in ionic liquids on electrical double layer structures and surface force using classical density functional approach," The Journal of Chemical Physics 142, 174704 (2015).
- ³⁴K. Komori and T. Terao, "Cluster-size distribution of ions in concentrated aqueous nacl solutions: Molecular dynamics simulations," Chemical Physics Letters 825, 140627 (2023).
- ³⁵D. Ribar, C. E. Woodward, S. Nordholm, and J. Forsman, "Cluster formation induced by local dielectric saturation in restricted primitive model electrolytes," J. Phys.Chem. Lett. **15**, 8326–8333 (2024).
- ³⁶M. Sedlak, "Large-scale supramolecular structure in solutions of low molar mass compounds and mixtures of liquids: I. light scattering characterization," The Journal of Physical Chemistry B 110, 4329–4338 (2006), pMID: 16509731, https://doi.org/10.1021/jp0569335.
- ³⁷M. Sedlak, "Large-scale supramolecular structure in solutions of low molar mass compounds and mixtures of liquids: Ii. kinetics of the formation and long-time stability," The Journal of Physical Chemistry B 110, 4339–4345 (2006), pMID: 16509732, https://doi.org/10.1021/jp056934x.
- ³⁸Z. Liao, A. Das, I. Ahmed, I. Abate, I. MacLaren, R. Beveridge, and K. Wynne, "Nucleation begins before supersaturation: glassy solute aggregates dominate solution structure," ChemRxiv (2025), chemRxiv preprint.
- ³⁹D. J. M. Irving, M. E. Light, M. P. Rhodes, T. Threlfall, and T. F. Headen, "A total scattering study of prenucleation structures in saturated aqueous magnesium sulfate – observation of extended clusters," Physical Chemistry Chemical Physics 25, 14898–14906 (2023).

- ⁴⁰Y. Georgalis, A. M. Kierzek, and W. Saenger, "Cluster formation in aqueous electrolyte solutions observed by dynamic light scattering," The Journal of Physical Chemistry B **104**, 3405–3406 (2000).
- ⁴¹È. O. Fetisov, C. J. Mundy, G. K. Schenter, C. J. Benmore, J. L. Fulton, and S. M. Kathmann, "Nanometer-scale correlations in aqueous salt solutions," The Journal of Physical Chemistry Letters 11, 2598–2604 (2020).
- ⁴²A. Shalit, S. Ahmed, J. Savolainen, and P. Hamm, "Terahertz echoes reveal the inhomogeneity of aqueous salt solutions," Nature Chemistry 9, 273–278 (2016).
- ⁴³ J. S. Straub, M. S. Nowotarski, J. Lu, T. Sheth, S. Jiao, M. P. A. Fisher, M. S. Shell, M. E. Helgeson, A. Jerschow, and S. Han, "Phosphates form spectroscopically dark state assemblies in common aqueous solutions," Proceedings of the National Academy of Sciences 120 (2022), 10.1073/pnas.2206765120.
- ⁴⁴A. R. Crothers, C. Li, and C. Radke, "A grahame triple-layer model unifies mica monovalent ion exchange, zeta potential, and surface forces," Advances in Colloid and Interface Science 288, 102335 (2021).
- ⁴⁵C. E. Woodward, "Density functional theory for inhomogeneous polymer solutions," J. Chem. Phys. **94**, 3183 (1991).
- ⁴⁶J. M. Wichert, H. S. Gulati, and C. K. Hall, "Binary hard chain mixtures i. generalized flory equations of state." J. Chem. Phys. 105, 7669 (1996).

- ⁴⁷J. Forsman and C. E. Woodward, "Surface forces at restricted equilibrium, in solutions containing finite or infinite semi-flexible polymers," Macromol 40, 8396 (2007).
- ⁴⁸S. Nordholm, J. Forsman, C. Woodward, B. Freasier, and Z. Abbas, Generalized Van der Waals Theory of Molecular Fluids in Bulk and At Surfaces (Elsevier, Amsterdam, 2018).
- $^{49}\mbox{Recall}$ that the implicit solvent imposes a uniform dielectric constant $\varepsilon_w.$
- ⁵⁰J. T. Edsall and J. J. Wyman, "Studies in the physical chemistry of betaines and related substances. i. studies of dielectric constants and apparent molal volume1," Journal of the American Chemical Society 57, 1964–1975 (1935), https://doi.org/10.1021/ja01313a063.
- ⁵¹R. Govrin, S. Tcherner, T. Obstbaum, and U. Sivan, "Zwitterionic osmolytes resurrect electrostatic interactions screened by salt," Journal of the American Chemical Society 140, 14206–14210 (2018), pMID: 30296829, https://doi.org/10.1021/jacs.8b07771.
- ⁵²D. Ribar, C. E. Woodward, and J. Forsman, "Exceptionally strong double-layer barriers generated by polyampholyte salt," The Journal of Physical Chemistry B **129**, 4241–4248 (2025), pMID: 40178092, https://doi.org/10.1021/acs.jpcb.5c00012.
- ⁵³C. E. Woodward and J. Forsman, "Density functional theory for polymer fluids with molecular weight polydispersity," Phys. Rev. Lett. **100**, 098301 (2008).